Polarization in Photon Absorption Experiments *

Peter Grabmayr [a] and Alexander Natter [a]
for the A2-Collaboration at MAMI, Mainz

[a] Physikalisches Institut der Universität Tübingen
Auf der Morgenstelle 14, D-72076 Tübingen, Germany

This contribution reports on new codes and new calculations of the linear polarization of real photons produced by coherent bremsstrahlung off a diamond crystal. The exploratory studies are performed at an electron energy of 120 MeV. Originally these programmes were developed for experiments in the photon enrgy range of 180 to 450 MeV in order to interpret polarization experiments at the MAMI accelerator which aim at the study of Nucleon-Nucleon Correlations. Measured asymmetries for the ^{4}He($\vec{\gamma}$,np) and the ^{4}He($\vec{\gamma}$,npp) reactions are presented.

1. Introduction

Polarization and asymmetry measurements play an increasingly important role in medium energy physics as they have provided a large amount of recent progress. Linearly polarized photons can be produced on a crystal by coherent bremsstrahlung. The regular structure of atoms within a coherence volume leads to an enhancement of radiation of polarized photons within a finite phase space. The cross section for production of bremsstrahlung on a crystal (cr) is composed of a coherent (co) and an incoherent (in) part

$$\sigma^{\mathrm{cr}} = \sigma^{\mathrm{co}} + \sigma^{\mathrm{in}} = \sigma_{\perp} + \sigma_{\|} + \sigma^{\mathrm{in}} ,$$

where σ is used as an abbreviation for the differential cross section. The incoherent cross section differential in photon energy k has a smooth $1/k$ energy dependence while the coherent cross section exhibits structures related to the periodicities of the lattice (see Fig. 1). The coherent part can be decomposed into two contributions, whose photon polarization vector is perpendicular ($\perp$) or parallel ($\|$) to the orientation of a reference plane defined by the incoming electron and the lowest reciprocal lattice vector of the crystal. Their difference determine the photon beam polarization P:

$$P = \sigma^{\mathrm{dif}}/\sigma^{\mathrm{cr}} = (\sigma_{\perp} - \sigma_{\|})/\sigma^{\mathrm{cr}} = \frac{\sigma_{\perp} - \sigma_{\|}}{\sigma_{\perp} + \sigma_{\|}} \left(1 - \frac{1}{R}\right) ,$$

where $R = \sigma^{\mathrm{cr}}/\sigma^{\mathrm{in}}$.

Based on the work by Timm [1] and the Göttingen group [2] we have improved the description of the incoherent as well as the coherent processes by use of (i) more recent realistic form factors and a realistic angular distribution and (ii) a more detailed description of the beam divergence, collimator function and multiple scattering within thick radiators.

*this work is supported by the DFG-Schwerpunkt SPP1034

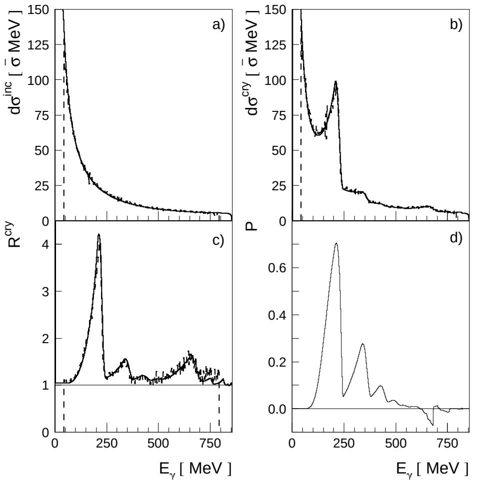

Figure 1. Comparison of measured and calculated bremsstrahlung spectra with different radiator. a) Ni radiator b) diamond radiator, c) ratio of diamond/nickel yield d) predicted polarization.

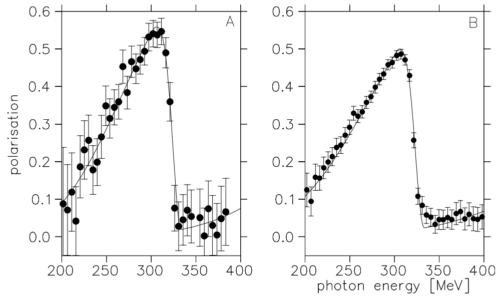

Figure 2. Comparison of measured and calculated polarization, obtained in the ^{4}He($\vec{\gamma}$,π°) experiment [2]. Two collimators with radii of 3 mm (left) and 5 mm (right) were used.

This work [4,5] produced two codes, one relies on the Monte-Carlo technique for a most precise calculation of all effects and a second one for quick surveys where some analytical expressions replaced the time consuming integrations. The accurate description of the photon polarization from a ^{4}He($\vec{\gamma}$,π°) experiment (Fig. 2) as well as the photon energy spectra for amorphous and crystalline radiators (see Fig. 1) gives the confidence for further predictions. Fig. 1 shows a comparison of electron spectra obtained at $E_\circ$=855 MeV on nickel and diamond radiators with our Monte Carlo predictions.

2. Linearly polarized photons at low energies

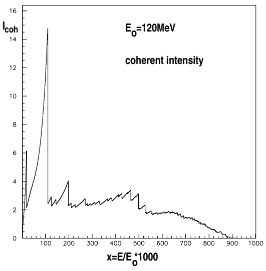

Figure 3. Calculated coherent intensity for $E_\circ$=120 MeV.

Systematic investigations at various electron energies demonstrated that a better selection of single lattice vectors can be achieved at higher electron energies than for lower ones. This fact originates from the very low transversal momentum transfer and the principal scaling proportionality of the coherent cross section with $E_\circ/a$, where $E_\circ$ is the electron energy and a specifies the size of a basic lattice cell. In contrast to the single structures in the coherent contributions at high energies one observes for a low energetic electron beam (see Fig. 3) a wealth of lattice vectors which satisfy the Laue condition. There are no crystals with significant smaller lattice cells available. No beam divergence and straggling in the radiator is considered in this particular calculation. For remedy we suggest to use thick crystals (100 μm) and moderate beam divergences (ε= 0.1 mrad$\times$0.5 mm). Both measures smear out the wealth of structures but still produce significant polarization.

Fig. 4 demonstrates for S-DALINAC energies (appropriate for the occasion we have chosen $E_\circ$=2$\times$60=120 MeV) that the photon range up to E_γ=35 MeV can be covered by

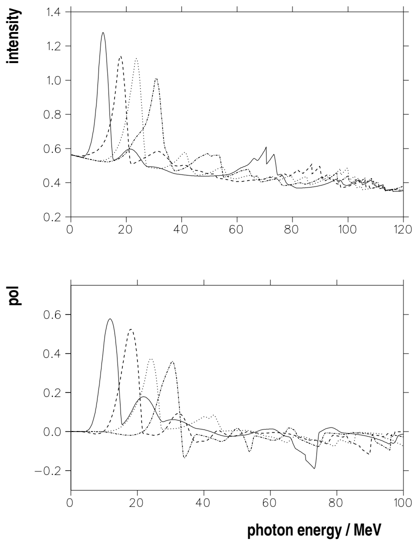

Figure 4. Four different crystal settings covering the low photon energy part.

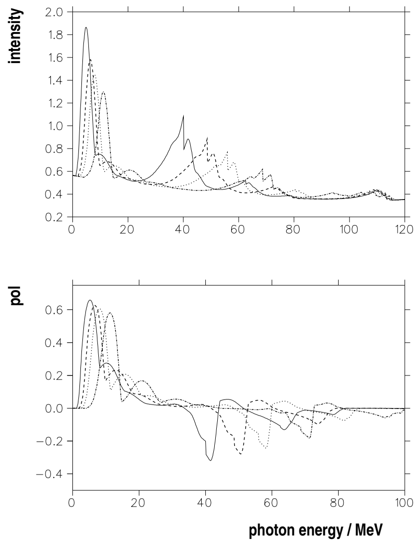

Figure 5. Four different crystal settings covering the high photon energy part.

four angular settings of the diamond using the $[02\bar{2}]$ lattice vector. The figures show the total intensity in the top panel and the polarization in the bottom one; the four settings are coded by different line styles. For the energy range $35<E_\gamma<70$ MeV the $[04\bar{4}]$ vector provides about 30% polarization, sufficiently large for experiments (Fig. 5).

3. Asymmetries in the ^{4}He($\vec{\gamma}$,np) reaction

The studies of the two-nucleon knockout reaction aim at the understanding of the short range nuclear force, i.e. nucleon-nucleon correlations in atomic nuclei. The *np* channel is sensitive also to the tensor part whereas the *pp* channels tests the central part only. Due to the transverse character of real photons the competing process of meson-exchange currents contribute strongly; isobaric currents and final-state interaction produce additional background contributions some of which can be separated by proper choice of kinematics. Polarization degrees of freedom are assumed [6] to be less affected by the competing processes. Multiple scattering or pion production leading to two detected nucleons will exhibit vanishing asymmetries.

Amongst other light nuclei ^{4}He has been chosen for its special features of (i) sitting at the border line between the few-body systems and 'real nuclei' (as defined by the universal behaviour of the total photoabsorption cross sections) and of (ii) being less affected by FSI than heavier nuclei studied sofar.

The experimental setup of the PiP/ToF experiments at the Glasgow tagger facility of the MAMI accelerator is described elsewhere (e.g. [7,8]). The reconstructed missing energy E_{2m} for two-nucleon emission - which is a measure of the excitation of the residual - is shown on logarithmic scale in Fig. 6(topped triangles). One notices the huge peak of the two-body breakup at E_{2m}=28 MeV followed by a tail extending to E_{2m}=170 MeV and a second structure around 250 MeV due to pion production. With small probability also *ppn* triple are recorded in the detector setup; their distribution (blue) does not show this low-E_{2m} peak. However, yields a sharp peak again, demonstrating that indeed the tail region of the E_{2m} distribution is due to relative energy in the residual *np* system.

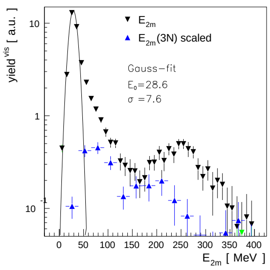

Figure 6. Comparison of two-body missing mass spectra for *pn*-pairs and detected *ppn*-triples.

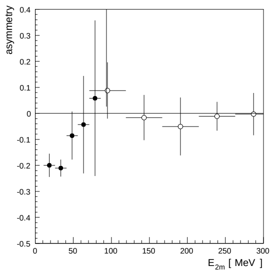

Figure 7. Asymmetry of missing energy (E_{2m}) in the photon range 170-400 MeV.

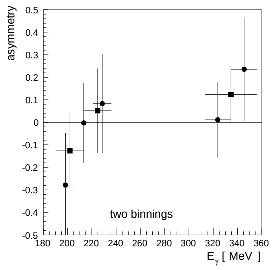

Figure 8. Asymmetry of the ^{4}He($\vec{\gamma}$,npp) reaction.

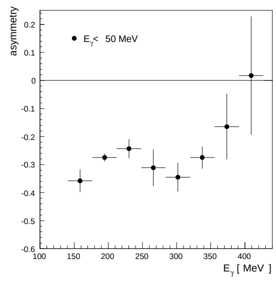

Figure 9. Asymmetry of the ^{4}He($\vec{\gamma}$,np) reaction for E_{2m} <50 MeV.

The determined asymmetries support the interpretation of sizeable negative polarization for low missing energies. (Fig. 7). The photon energy dependence of the asymmetry for E_{2m} <50 MeV (Fig. 9) is different from that for ^{12}C and for D. The change of slope between 200 and 300 MeV was predicted by J. Ryckebusch [9] and is supposedly due to tensor correlation, which must be verified be a more detailed calculation. Finally, the asymmetry for the 3-particle reaction (Fig. 8) is slightly positive; clearly different from that for two-body breakup.

4. Conclusion

The new Monte Carlo code enables a precise prediction of the structure obtained from coherent bremsstrahlung. For case studies a fast analytical version of the code is available which still is accurate to ∼2%. It is demonstrated that the use of linearly polarized photons improves the separation of two- and three-body processes in the photoabsorption on light nuclei. Calculations of asymmetries are in progress.

REFERENCES

1. U. Timm, Fortschritte der Physik **17** (1969) 765
2. F. Rambo *et al.*, Phys. Rev. **C58** (1998) 489
3. H. Bilokon *et al.*, Nucl. Instr. Methods **204** (1983) 299
4. A. Natter, contrib. paper to 4^{th}Workshop on electromagnetically induced Two-Hadron Emission, Granada 1999, ISBN: 84-699-1645-9
5. A. Natter *et al.*, Nucl. Instr. Methods, to be published `http://www.pit.physik.uni-tuebingen.de/grabmayr/software/software.html`
6. S. Boffi *et al.*, Nucl. Phys. **A564** (1983) 473
7. P. Grabmayr, Prog. Part. Nucl. Phys. **44** (2000) 113
8. F.A. Natter, Prog. Part. Nucl. Phys. **44** (2000) 461
9. J. Ryckebusch, priv. comm